

Scale Invariant Geometry for Nonrigid Shapes*

Yonathan Aflalo[†], Ron Kimmel[‡], and Dan Raviv[‡]

Abstract. In nature, different animals of the same species frequently exhibit local variations in scale. New developments in shape matching research thus increasingly provide us with the tools to answer such fascinating questions as the following: How should we measure the discrepancy between a small dog with large ears and a large one with small ears? Are there geometric structures common to both an elephant and a giraffe? What is the morphometric similarity between a blue whale and a dolphin? Currently, there are only two methods that allow us to quantify similarities between surfaces which are insensitive to deformations in size: scale invariant local descriptors and global normalization methods. Here, we propose a new tool for shape exploration. We introduce a scale invariant metric for surfaces that allows us to analyze nonrigid shapes, generate locally invariant features, produce scale invariant geodesics, embed one surface into another despite changes in local and global size, and assist in the computational study of intrinsic symmetries where size is insignificant.

Key words. scale invariant, Laplace–Beltrami, shape analysis

AMS subject classifications. 53B21, 58D17

DOI. 10.1137/120888107

1. Introduction. The study of invariants in shape analysis began with the application of differential signatures—previously used only in differential geometry for planar curves subject to projective transformations—to contours representing the boundaries of objects in images [12, 13, 14, 17, 45, 63]. Although analytically elegant, differential signatures are somewhat messy; the many parameters associated with projective transformations require estimating a large number of derivatives. In response, some have considered simpler transformations—for example, similarity (scale) and affine transformations—and others have tried replacing local differential signatures with global invariants on a local scale [12, 13, 14, 16, 17, 21]. Bruckstein, Rivlin, and Weiss [15] first introduced scale space signatures, whereby a location is parameterized by a factor indicating how far one should move from the point of interest. Another approach, known as semidifferential invariants, reduces the number of derivatives required for generating local invariants by using external matching points [18, 39, 45, 58, 59]. Bruckstein et al. [12] combined both of these methods in their derivation of local, nondifferential invariants with external matching points that reduce the number of derivatives. Extending support to a shape as a whole ultimately aids planar shape recognition, despite sacrificing resistance to occlusions, as demonstrated in [11, 33, 41, 42]. Meanwhile, efforts were also made to simplify

*Received by the editors August 14, 2012; accepted for publication (in revised form) May 13, 2013; published electronically August 22, 2013. This research was supported by the Israel Science Foundation (grant 1031/12) and by the E. and J. Bishop Research Fund.

<http://www.siam.org/journals/siims/6-3/88810.html>

[†]Faculty of Electrical Engineering, Technion University, Haifa 32000, Israel (yaflo@cs.technion.ac.il).

[‡]Faculty of Computer Science, Technion University, Haifa 32000, Israel (ron@cs.technion.ac.il, darav@cs.technion.ac.il).

images while maintaining invariance by using geometric diffusion of the level sets of the image in gray level [1, 32, 56].

Lowe's introduction of the *scale invariant feature transform* (SIFT) [36] represents a milestone in the field of image analysis. His method compensates for distortions resulting from images taken at various distances by sampling the blur (and scale) space. In the same vein, Morel and Yu [40] developed affine-SIFT (ASIFT) to sample the space of affine transformations [40].

Digital photometric images allow us to project the world into numbers that we can readily process. Through new geometric sensors known as three-dimensional scanners, we can now also capture the geometric structures of objects. By incorporating SIFT-like descriptors into the surface recognition process, we can analyze, compare, and understand this new geometric data. One such descriptor uses heat diffusion on the inspected surface, instead of Lowe's diffusion in the image domain. This feature, known as the *heat kernel signature* (HKS), measures the rate of virtual heat dissipation from a surface point [57]. The short time realization of this feature is trivially related to the Gaussian curvature. Many other differential operators have been proposed as local descriptors, as in [66]. Notably, [54] proposes the related similarity invariant curvature for surfaces using the ratio between the magnitudes of the surface principal curvatures. Finally, [53] proposes spectral analysis as a means of choosing the points to consider.

Chazal et al. [19] explore the treatment of signatures as structures in their own metric spaces. These tools, first developed to compare one shape to another, were also found to be useful in exploring intrinsic isometries by computationally mapping a surface to itself (e.g., [48, 49] and, later, [44]). Most nearly isometric area preserving deformations are explored in [35, 64]. The former introduces bending energy to the field, while the latter is strictly intrinsic. Other notable contributions to the field of shape and surface matching include [30, 60].

An important aspect of any shape correspondence measurement method is the set of transformations and deformations it can handle. Thus far, nonrigid shapes have been treated as metric spaces characterized by various definitions from theoretical metric geometry [8, 37]. Shapes have been embedded into elementary spaces in order to compare and match structures using relatively simple procedures, at the cost of drastic simplifications and compromises. These target spaces include Euclidean spaces [26, 55], spherical domains [7, 8], conformal disks and spheres [34], and topological graphs [27, 28, 61], to name just a few. Instead of using exact point-to-point matching for efficient shape recognition, [5] uses local features, aggregated as a bag of words as a signature for efficient shape recognition.

Choosing an appropriate metric is crucial to developing shape analysis methods that are resistant to transformations. Researchers have been using Euclidean distances [3, 20], geodesic distances [6, 8, 26, 29, 37, 43], diffusion distances [9, 50], and affine invariant versions of these to compare and match shapes [52]. The magnitude of the Fourier transform applied to the first derivative w.r.t. the logarithmic scale (time) of the log of HKSs was shown to produce scale invariant local descriptors [10].¹ Digne et. al define scale space meshing of raw data

¹The scale invariant heat kernel signature SI-HKS(s, ξ) of the surface point s at time t is defined as a function of the HKS by SI-HKS(s, ξ) = $|\mathcal{F}(\frac{d}{d\eta} \lg(\text{HKS}(s, \eta)))|$, where \mathcal{F} denotes the Fourier transform, the HKS(s, t) is defined in (5.1), and $\eta = \log(t)$.

points in [24]. Still, though the signature is local, the invariant by which it is constructed relates to global rather than local scaling. Other nondifferential global invariants can be found in normalization methods like the commute time distance [47]. Once correspondence between two objects is achieved, the same measures can then be used to deform, morph, or warp one shape into another [31].

In section 2, we introduce an invariant metric for surfaces as a new solution to the scale invariant matching problem. In section 3 we demonstrate the benefit of plugging the new metric into the diffusion distance framework. We discuss implementation considerations with the diffusion formulation in section 4. Finally, in section 5, we demonstrate the framework's potential through various test cases involving local and global scale variations as well as nonrigid deformations of shapes. It is shown that the proposed intrinsic measures are efficient to compute as well as robust to noise, and are invariant to local and global scaling and isometries.

2. Problem formulation. Consider $S(u, v)$, a parametrized surface $S : \Omega \subset \mathbb{R}^2 \rightarrow \mathbb{R}^3$. We can measure the length of a parametrized curve C in S using either the Euclidean arc-length s or a general parametrization p . The length is given by

$$\begin{aligned} l(C) &= \int_{C \in S} ds = \int_C |C_p| dp = \int_C |S_u u_p + S_v v_p| dp \\ &= \int_C \sqrt{|S_u|^2 du^2 + 2\langle S_u, S_v \rangle dudv + |S_v|^2 dv^2}, \end{aligned}$$

from which we have the usual metric definition of infinitesimal distances on a surface,

$$ds^2 = g_{ij} d\omega^i d\omega^j,$$

where we use the Einstein summation convention, $\omega^1 = u$, $\omega^2 = v$, and $g_{ij} = \langle S_{\omega^i}, S_{\omega^j} \rangle$.

Let us first consider the simple case where $S = \mathbb{R}^2$. A scale invariant arc-length for a planar curve C is given by $d\tau = |\kappa| ds$, where $|\kappa| = |C_{ss}|$ is the scalar curvature magnitude. The invariance can be easily explained by the fact that the curvature is defined by the rate of change of the angle θ of the tangent vector w.r.t. the Euclidean arc-length, namely

$$\frac{d\theta}{ds} = \kappa,$$

from which we have the scale invariant measure $d\theta = \kappa ds$ or in its monotone arc-length form $d\tau = |\kappa| ds$.

The next challenge would be dealing with a less trivial surface. By its definition, the curvature of a planar curve is inversely proportional to the radius of the osculating circle $\kappa = \rho^{-1}$ at any given point along the curve. Thus, for a curve on a nonflat surface we need to find such a scalar that would cancel the scaling effect. Recall that for surfaces there are two principal curvatures κ_1 and κ_2 at each point. These scalars, or combinations thereof, could serve for constructing normalization factors that modulate the Euclidean arc-length on the surface for scale invariance. This is the case for

$$d\tau = |\kappa_1| ds = \frac{1}{|\rho_1|} ds \quad \text{or} \quad d\tau = |\kappa_2| ds = \frac{1}{|\rho_2|} ds.$$

We could also define similarity or scale invariant arc-length using the mean curvature $2H = \kappa_1 + \kappa_2$ and the Gaussian curvature $K = \kappa_1\kappa_2$. Thus,

$$d\tau = \left| \frac{K}{H} \right| ds = \frac{2}{|\rho_1 + \rho_2|} ds$$

would be similarity (scale) invariant, as would

$$d\tau = \sqrt{|K|} ds = \frac{1}{\sqrt{|\rho_1\rho_2|}} ds.$$

Yet, of the above possible options, only the last one is intrinsic in the sense that it is also invariant to isometric transformations of the surface. We therefore consider the scale invariant isometric metric

$$(2.1) \quad \tilde{g}_{ij} = |K| \langle S_{\omega^i}, S_{\omega^j} \rangle,$$

so that

$$d\tau^2 = |K| (\langle S_u, S_u \rangle du^2 + 2\langle S_u, S_v \rangle dudv + \langle S_v, S_v \rangle dv^2),$$

as our candidate for a scale invariant arc-length.

Given the surface normal

$$\vec{n} = \frac{S_u \times S_v}{|S_u \times S_v|},$$

the second fundamental form is defined by

$$b_{ij} = \langle S_{\omega^i\omega^j}, \vec{n} \rangle = \frac{\det(S_{\omega^i\omega^j}, S_u, S_v)}{\sqrt{g}},$$

from which we have the Gaussian curvature $K \equiv b/g$, where $b = \det(b_{ij})$ and $g = \det(g_{ij})$.

Using the above notation we can write our similarity (scale) invariant metric \tilde{g}_{ij} as a function of the regular metric g_{ij} and the second fundamental form b_{ij} . Recall that the metric structure is positive definite, that is, $g > 0$. It allows us to write

$$\tilde{g}_{ij} = |K| g_{ij} = \frac{|b|}{g} g_{ij}.$$

It is interesting to note that the recent affine invariant metric explored in [51] could be written using similar notation as

$$g_{ij}^{\text{equiaffine}} = |K|^{-1/4} b_{ij} = \left(\frac{g}{|b|} \right)^{1/4} b_{ij},$$

projected onto a positive definite metric-matrix. The equiaffine intrinsic metric can be coupled with the scale invariant one to produce a full affine invariant metric for surfaces given by

$$g_{ij}^{\text{affine}} = |K^{\text{equiaffine}}| g_{ij}^{\text{equiaffine}} = |K^{\text{equiaffine}}| \left(\frac{g}{|b|} \right)^{1/4} b_{ij},$$

where the Gaussian curvature is extracted from the affine invariant metric, that is, $K^{\text{equiaffine}} = b^{\text{equiaffine}}/g^{\text{equiaffine}}$ and $|g^{\text{equiaffine}}| = \sqrt{g|b|}$. Note that as we have been using intrinsic measures to construct this metric, it would also be invariant to isometries within that space.

The following theorem is similar to the one that Raviv and Kimmel prove in [52].

Theorem 2.1. *Given a parametrized surface $S(u, v) : \Omega \subset \mathbb{R}^2 \rightarrow \mathbb{R}^3$, the geometric quantity*

$$\tilde{g}_{ij} = |K| \langle S_{\omega^i}, S_{\omega^j} \rangle$$

is both scale and isometric invariant.

Proof. Considering the surface $\bar{S} = \alpha S$, we have

$$\langle \bar{S}_{\omega^i}, \bar{S}_{\omega^j} \rangle = \alpha^2 \langle S_{\omega^i}, S_{\omega^j} \rangle,$$

and the Gaussian curvature can be expressed in terms of the first and second fundamental forms, as follows:

$$K = \frac{b_{11}b_{22} - b_{12}^2}{g_{11}g_{22} - g_{12}^2},$$

where g_{11} , g_{12} , g_{22} are the coefficients of the first fundamental form and b_{11} , b_{12} , b_{22} are the coefficients of the second fundamental form. We readily have

$$\begin{aligned} g_{ij} &= \langle S_{\omega^i}, S_{\omega^j} \rangle, \\ b_{ij} &= \langle S_{\omega^i, \omega^j}, \vec{n} \rangle. \end{aligned}$$

It is easy to show that

$$\begin{aligned} \bar{g}_{ij} &= \alpha^2 g_{ij}, \\ \bar{b}_{ij} &= \alpha b_{ij}, \end{aligned}$$

where \bar{g}_{11} , \bar{g}_{12} , \bar{g}_{22} , \bar{b}_{11} , \bar{b}_{12} , \bar{b}_{22} , \bar{K} correspond to fundamental forms of the scaled manifold \bar{S} . Then

$$\bar{K} = \frac{\alpha^2}{\alpha^4} K = \frac{1}{\alpha^2} K,$$

and

$$\tilde{\bar{g}}_{ij} = |\bar{K}| \langle \bar{S}_{\omega^i}, \bar{S}_{\omega^j} \rangle = \frac{1}{\alpha^2} |K| \alpha^2 \langle S_{\omega^i}, S_{\omega^j} \rangle = \tilde{g}_{ij}.$$

Finally, since both quantities $|K|$ and $\langle S_{\omega^i}, S_{\omega^j} \rangle$ are isometric invariant, the tensor is both isometric and scale invariant. ■

Equation (2.1) defines a positive semidefinite matrix. The resulting tensor is bilinear, symmetric, and positive semidefinite, but it does not satisfy the property of nondegeneration since \tilde{g} vanishes where the curvature vanishes. We therefore regularize the tensor according to

$$\tilde{g}_{ij} = \left(\sqrt{K^2 + \epsilon^2} \right) \langle S_{\omega^i}, S_{\omega^j} \rangle.$$

This tensor is nondegenerate and defines an isometric and scale invariant metric up to $O(\epsilon)$.

The modulation of the metric tensor by a Gaussian curvature obviously makes flat regions weigh significantly less than curved domains. When examining articulated objects in nature

we notice that the limbs are connected with generalized cylinders–like structures for which the local geometry is that of a flat manifold with vanishing Gaussian curvature. From a theoretical point of view this would appear, at first glance, to be a deficiency of the proposed framework—flat regions would simply shrink to points in the new metric. Yet, recall that the interesting regions, from a scale invariant point of view, are exactly those at which there is an effective Gaussian curvature.

3. Scale invariant diffusion geometry. Diffusion geometry was introduced by Coifman and Lafon [22]. It uses the Laplace–Beltrami operator $\Delta_g \equiv -\frac{1}{\sqrt{g}}\partial_i\sqrt{g}g^{ij}\partial_j$ of the surface as a diffusion or heat operator by which distances are measured. In fact, *diffusion maps* embed a given shape into the Euclidean space spanned by the eigenfunctions of the shape’s Laplace–Beltrami operator [2]. Euclidean distances in the eigenspace are diffusion distances on the actual surface. Here, without giving up its isometric nature w.r.t. the metric, we use the operator $\Delta_{\bar{g}}$ to construct a scale invariant diffusion geometry. The diffusion distance between two surface points $s, \hat{s} \in S$ is given by the surface integral over the difference between two heat profiles dissipating from two sources, one located at s and the other at \hat{s} . The heat profile on the surface from a source located at s , after heat has dissipated for time t , is given by the heat kernel

$$h_{s,t}(\hat{s}) = \sum_i e^{-\lambda_i t} \phi_i(s) \phi_i(\hat{s}),$$

where ϕ_i and λ_i are the corresponding eigenfunctions and eigenvalues of $\Delta_{\bar{g}}$, which satisfy $\Delta_{\bar{g}}\phi_i = \lambda_i\phi_i$. Obviously, $h_{s,t}(\hat{s})$ satisfies the heat equation as

$$\frac{\partial h}{\partial t} = \sum_i -\lambda_i e^{-\lambda_i t} \phi_i(s) \phi_i(\hat{s}),$$

and

$$\Delta_{\bar{g}}h = \sum_i e^{-\lambda_i t} \Delta_{\bar{g}}\phi_i(s) \phi_i(\hat{s}) = \sum_i e^{-\lambda_i t} \lambda_i \phi_i(s) \phi_i(\hat{s}) = -\frac{\partial h_{s,t}(\hat{s})}{\partial t}.$$

The diffusion distance is then defined by

$$\begin{aligned} d_{g,t}^2(s, s') &= \|h_{s,t} - h_{s',t}\|_{\bar{g}}^2 \\ &= \int_S (h_{s,t}(\hat{s}) - h_{s',t}(\hat{s}))^2 da(\hat{s}) \\ (3.1) \qquad &= \sum_i e^{-2\lambda_i t} (\phi_i(s) - \phi_i(s'))^2. \end{aligned}$$

One can prove that $d_{g,t}$ is indeed a distance as it satisfies the following three properties [23]:

1. Nonnegativity: $d(s, s') \geq 0$. As the argument in the integral is never negative, the integral cannot be negative.
2. Indistinguishability: $d(s, s') = 0$ if and only if $s = s'$.
 - (a) If $s = s'$, then certainly $\phi_i(s) = \phi_i(s')$ for all i . Therefore, $\phi_i(s) - \phi_i(s') = 0$ for all i , and the summation defines the distance to be zero.
 - (b) If $d(s, s') = 0$, we have

$$\sum_i e^{-2\lambda_i t} (\phi_i(s) - \phi_i(s'))^2 = 0.$$

As the summation is over nonnegative terms, the sum vanishes if and only if each term is equal to zero. Thus, $\phi_i(s) - \phi_i(s') = 0$ for every i . We next prove that this implies $s = s'$.

The eigenfunctions $\{\phi_i\}$ form a complete orthonormal basis, which allows us to express any function f as $f = \sum_i \langle f, \phi_i \rangle \phi_i$, where $\langle f, \phi_i \rangle = \int \phi_i f dx$ is the inner product in that basis. Consider, for example, $f = \delta_\epsilon(x - s) - \delta_\epsilon(x - s')$, where $\delta_\epsilon(x) = \frac{1}{(4\pi\epsilon)^d} e^{-x^2/4t}$ such that $\lim_{\epsilon \rightarrow 0} \delta_\epsilon(x) = \delta(x)$ is the delta function. f is smooth and continuous everywhere, and we readily have that

$$\lim_{\epsilon \rightarrow 0} \int \phi_i f dx = \int \lim_{\epsilon \rightarrow 0} \phi_i \delta_\epsilon(x - s) dx - \int \lim_{\epsilon \rightarrow 0} \phi_i \delta_\epsilon(x - s') dx = \phi_i(s) - \phi_i(s') = 0$$

for all i . Thus, the decomposition of f is zero for all i ; this is the case if and only if $f = 0$, that is, if $\delta(x - s) = \delta(x - s')$, which implies $s = s'$.

3. Triangle inequality: $d(s_1, s_2) \leq d(s_1, s_3) + d(s_3, s_2)$.

$$\begin{aligned} d^2(s_1, s_2) &= \sum_i e^{-2\lambda_i t} (\phi_i(s_1) - \phi_i(s_2))^2 = \sum_i (e^{-\lambda_i t} \phi_i(s_1) - e^{-\lambda_i t} \phi_i(s_2))^2 \\ &= \sum_i ((e^{-\lambda_i t} \phi_i(s_1) - e^{-\lambda_i t} \phi_i(s_3)) + (e^{-\lambda_i t} \phi_i(s_3) - e^{-\lambda_i t} \phi_i(s_2)))^2. \end{aligned}$$

Let $a_i = e^{-\lambda_i t} \phi_i(s_1) - e^{-\lambda_i t} \phi_i(s_3)$ and $b_i = e^{-\lambda_i t} \phi_i(s_3) - e^{-\lambda_i t} \phi_i(s_2)$. Then, we have

$$\sum_i |a_i + b_i|^2 \leq \sum_i (|a_i| + |b_i|) |a_i + b_i| = \sum_i |a_i| |a_i + b_i| + \sum_i |b_i| |a_i + b_i|$$

and, by Holder's inequality,

$$\sum_i |a_i| |a_i + b_i| \leq \left(\sum_i |a_i|^2 \right)^{1/2} \left(\sum_i |a_i + b_i|^2 \right)^{1/2},$$

and similarly for the term in b_i . Combining the common factors, we arrive at

$$\sum_i |a_i + b_i|^2 \leq \left(\sum_i |a_i + b_i|^2 \right)^{1/2} \left(\left(\sum_i |a_i|^2 \right)^{1/2} + \left(\sum_i |b_i|^2 \right)^{1/2} \right)$$

and, thus,

$$\left(\sum_i |a_i + b_i|^2 \right)^{1/2} \leq \left(\sum_i |a_i|^2 \right)^{1/2} + \left(\sum_i |b_i|^2 \right)^{1/2}.$$

Substituting for a_i and b_i , we have

$$d(s_1, s_2) = \left(\sum_i |e^{-\lambda_i t} \phi_i(s_1) - e^{-\lambda_i t} \phi_i(s_2)|^2 \right)^{1/2}$$

$$\begin{aligned} &\leq \left(\sum_i |e^{-\lambda_i t} \phi_i(s_1) - e^{-\lambda_i t} \phi_i(s_3)|^2 \right)^{1/2} + \left(\sum_i |e^{-\lambda_i t} \phi_i(s_3) - e^{-\lambda_i t} \phi_i(s_2)|^2 \right)^{1/2} \\ &= d(s_1, s_3) + d(s_3, s_2), \end{aligned}$$

proving the inequality.

Integrating over the parameter t of the diffusion distance constructed with the regular metric g , one can obtain a global scale invariant diffusion distance [47]. This measure, also known as the commute time distance, is defined by

$$(3.2) \quad d_{\text{CT}}^2(s, s') = \int_0^\infty d_{g,t}^2(s, s') dt = \sum_i \frac{1}{2\lambda_i} (\phi_i(s) - \phi_i(s'))^2.$$

This is indeed an elegant setting for global scale invariance derived from the regular metric g . Yet, our goal is a bit more ambitious, that is, a measure that would be invariant to both local and global scale deformations. Here, by local we refer to parts of the shape that are connected by generalized cylinders. Next, we redefine the surface geometry so that it is both scale invariant in a differential fashion and stable by the integral averaging nature of the diffusion geometry. To that end, our new scale invariant differential geometric structure \tilde{g} is integrated within the diffusion distance framework.

4. Implementation considerations. In our experiments we assume a triangulated surface. We follow the decomposition of the Laplace–Beltrami diffusion operator proposed in [51]. In order to compute diffusion distances we need the eigenfunctions and eigenvalues of the scale invariant operator $\Delta_{\tilde{g}}$. For this purpose we could use the finite element method for triangulated surfaces; see [25].

The weak form of the eigendecomposition $\Delta_{\tilde{g}}\phi = \lambda\phi$ is given by

$$(4.1) \quad \int_S \psi_k \Delta_{\tilde{g}}\phi \, da = \lambda \int_S \psi_k \phi \, da,$$

where $\{\psi_k\}$ is a sufficiently smooth basis of $L^2(S)$, in our case first order finite element functions, and $da = \sqrt{\tilde{g}}dudv$ is a surface area element w.r.t. the metric \tilde{g} . The finite element function ψ_k is equal to one at the surface vertex k and decays linearly to zero in its 1-ring. The number of basis elements is thus equal to the number of vertices in our triangulated surface. Assuming vanishing boundary conditions, we readily have that

$$\begin{aligned} \int_S \psi_k \Delta_{\tilde{g}}\phi \, da &= \int_S \langle \nabla \psi_k, \nabla \phi \rangle_{\tilde{g}} \, da \\ &= \int_S \tilde{g}^{ij} (\partial_i \phi) (\partial_j \psi_k) \, da \\ (4.2) \quad &= \lambda \int_S \psi_k \phi \, da. \end{aligned}$$

Approximating the eigenfunction ϕ as a linear combination of the finite elements $\phi = \sum_l \alpha_l \psi_l$ leads to

$$\int_S \tilde{g}^{ij} \left(\partial_i \sum_l \alpha_l \psi_l \right) (\partial_j \psi_k) \, da = \sum_l \alpha_l \int_S \tilde{g}^{ij} (\partial_i \psi_l) (\partial_j \psi_k) \, da,$$

which should be equal to

$$(4.3) \quad \lambda \int_S \psi_k \sum_l \alpha_l \psi_l da = \lambda \sum_l \alpha_l \int_S \psi_l \psi_k da.$$

We thus need to solve for α_l that satisfy

$$(4.4) \quad \sum_l \alpha_l \underbrace{\int_S \tilde{g}^{ij}(\partial_i \psi_l)(\partial_j \psi_k) da}_{a_{kl}} = \lambda \sum_l \alpha_l \underbrace{\int_S \psi_l \psi_k da}_{b_{kl}},$$

or, in matrix form, $\mathbf{A}\alpha = \lambda\mathbf{B}\alpha$, defined by the above elements.

Another option is to numerically approximate the Laplace–Beltrami operator on the triangulated mesh and therein compute its eigendecomposition. There are many ways to approximate $\Delta_{\tilde{g}}$; see [62] for an axiomatic analysis of desired properties and possible realizations, and [46] for the celebrated cotangent weights approach. A comprehensive and useful introduction to geometric quantities approximation on triangulated surfaces can be found in [38]. We define the scale invariant cotangent weight by computing the cotangent weight of a scaled version of the mesh. Each triangle is scaled by the Gaussian curvature and then is used to compute the Laplace–Beltrami operator. We define the discrete scale invariant Laplace–Beltrami as

$$(4.5) \quad L = K^{-1}A^{-1}W,$$

where A represents the diagonal matrix whose i th component along the diagonal is the sum of the areas of every triangle that contains vertex i . K represents the discrete Gaussian curvature computed by [65] and regularized by

$$|K_i| = \sqrt{\left(\frac{3(2\pi - \sum_j \gamma_j^i)}{A_{ii}}\right)^2 + \epsilon}.$$

Here, γ_j^i is the angle at vertex i of the j th triangle that contains vertex i , and W is the classic cotangent weight matrix

$$W_{ij} = \begin{cases} \sum_{(i,j) \in E} (\cot \alpha_{ij} + \cot \beta_{ij}) & \text{if } i = j, \\ -(\cot \alpha_{ij} + \cot \beta_{ij}) & \text{if } i \neq j, (i,j) \in E, \end{cases}$$

where α_{ij} and β_{ij} are shown in Figure 1 and E is the set of all edges in our triangulated surface.

5. Experimental results. The first experiment demonstrates the invariance of the eigenfunctions of the Laplace–Beltrami operator w.r.t. the new metric \tilde{g} . Figures 2 and 3 present the first eigenfunctions, ϕ_1, ϕ_2, \dots , texture mapped on the surface using the usual metric $g_{ij} = \langle S_{\omega^i}, S_{\omega^j} \rangle$ and the scale invariant metric $\tilde{g}_{ij} = |K|g_{ij}$. The upper row of each frame

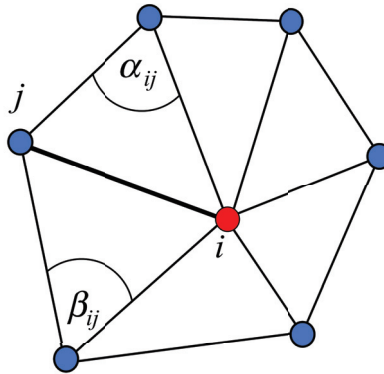


Figure 1. Cotangent weight.

shows the original surface, while the second row presents a deformed surface using isotropic inhomogeneous distortion field in space (local scales). Color represents the value of the eigenfunction at each surface point.

We next experiment with scale invariant heat kernel signatures [5, 57]. The heat kernel signature (HKS) at a surface point is a linear combination of all eigenfunctions given by

$$(5.1) \quad \text{HKS}(s, t) = h_{s,t}(s) = \sum_i e^{-\lambda_i t} \phi_i^2(s)$$

at that point. Figure 4 illustrates the invariance of the HKS when, in the top frame, it is texture mapped onto a centaur and its locally scaled version and, in the bottom frame, onto a normal horse and its distorted image—a horse with enlarged head that looks like a mule. Figure 5 displays the inconsistency of corresponding signatures with the regular metric (left) and the consistency achieved with the invariant metric (right). The signatures were extracted at three points as indicated in the figure: two finger tips (one on the right and one on the left hand of the centaur) and the horseshoe of the front left leg. In the graphs, the signature value at each time t is scaled w.r.t. the integral of the signatures at that time over the (invariant) surface area, i.e., $\text{HKS}(s, t) / \int_S \text{HKS}(s, t) da(s)$, as done in [57] for presentation purposes. As can be observed, the proposed metric produces invariant nontrivial informative signatures.

Next, we extract Voronoi diagrams for 30 points selected by the farthest point sampling strategy, using the tip of the nose as the first point. In this example, length is measured using diffusion distance with either a regular metric or the invariant one. Yet again, the invariant metric produces the expected result: the correspondence between the two surfaces is independent of the local scaling deformations. This is obviously not the case for the regular metric, as shown in Figure 6.

We can match two surfaces by embedding one surface into another, a method known as the *generalized multidimensional scaling* (GMDS) [6, 8]. Given two surfaces S and Q , the idea is to minimize for the mapping $\rho : S \rightarrow Q$ such that we solve for

$$\arg_{\rho} \min \max_{s, s' \in S} \|d_S(s, s') - d_Q(\rho(s), \rho(s'))\|.$$

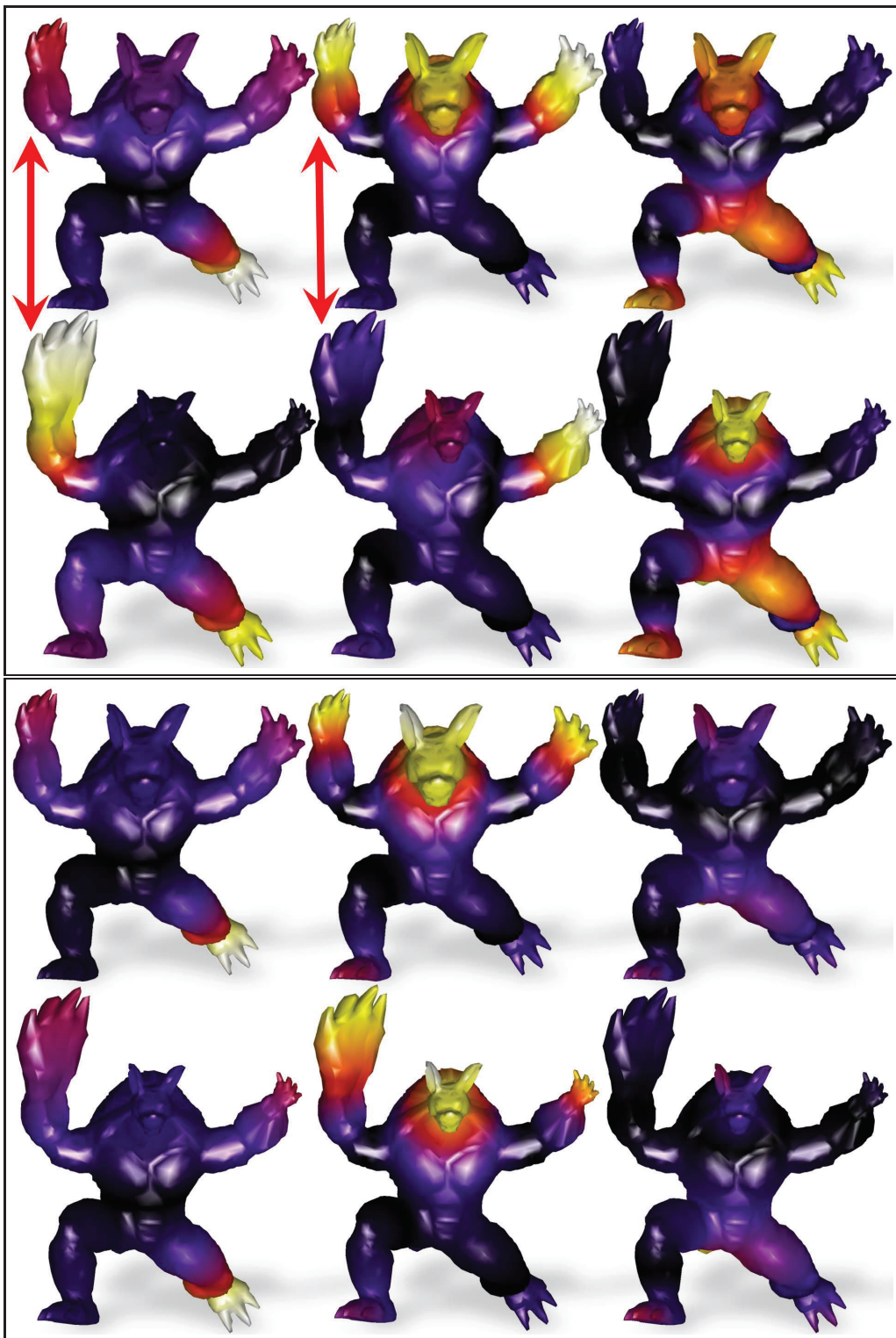


Figure 2. Three eigenfunctions of Δ_g (top) and the invariant version $\Delta_{\bar{g}}$ (bottom) for the armadillo with local scale distortions. Unlike the regular metric, the scale invariant metric preserves the correspondence between the matching eigenfunctions.

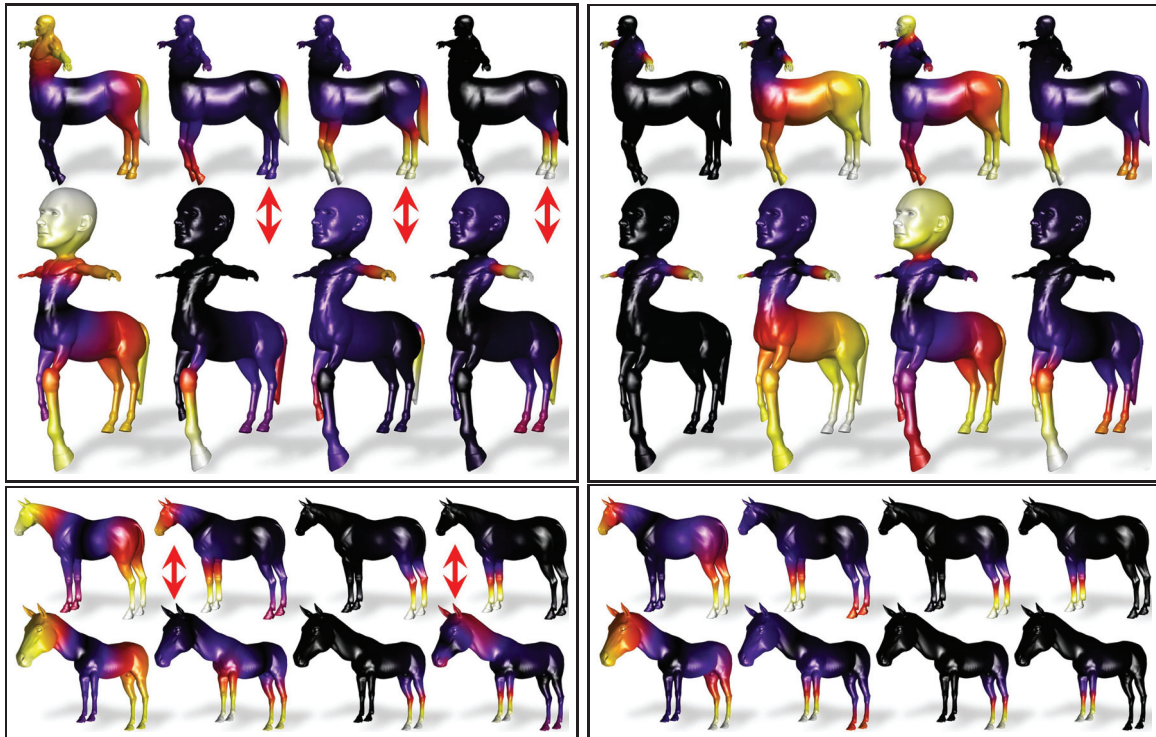


Figure 3. Four eigenfunctions of Δ_g (left) and the invariant version $\Delta_{\bar{g}}$ (right) for the centaur and a horse with local scale distortions. Unlike the regular metric, the scale invariant metric preserves the correspondence between the matching eigenfunctions.

The matching result for distances measured with the regular metric is demonstrated by the top two images of Figure 7, and the invariant version with much better correspondences is exhibited by the bottom images.

Finally, we experimented with HKSs computed with the proposed metric within the Shape-Google recognition framework applied to the SHREC'10 shape retrieval benchmark. That database is the only one in which there are supposed to be local scale variations. In fact, the distortions in that benchmark appear like dilation operations rather than scaling. Still, Table 1 demonstrates that the proposed framework can handle even these deformations while being robust to articulations referred to as isometries in the table, as well as topological noise that is handled by the diffusion part of the signature. The results are comparable to SG3 (relating to the SI-HKS of [10]) in the SHREC'10 framework [4].

6. Conclusions. We introduced a new metric that gracefully handles changes in size at virtually any scale—local (at shape parts connected with developable surfaces) to global changes as well as articulations that have relatively small effects on the Gaussian curvature. The proposed metric was integrated within the diffusion geometry and used to construct heat time kernels, which are, in fact, semidifferential scale invariant signatures for surfaces. Our future plans are to use the proposed measures and computational tools to study the geometric relations between objects in nature.

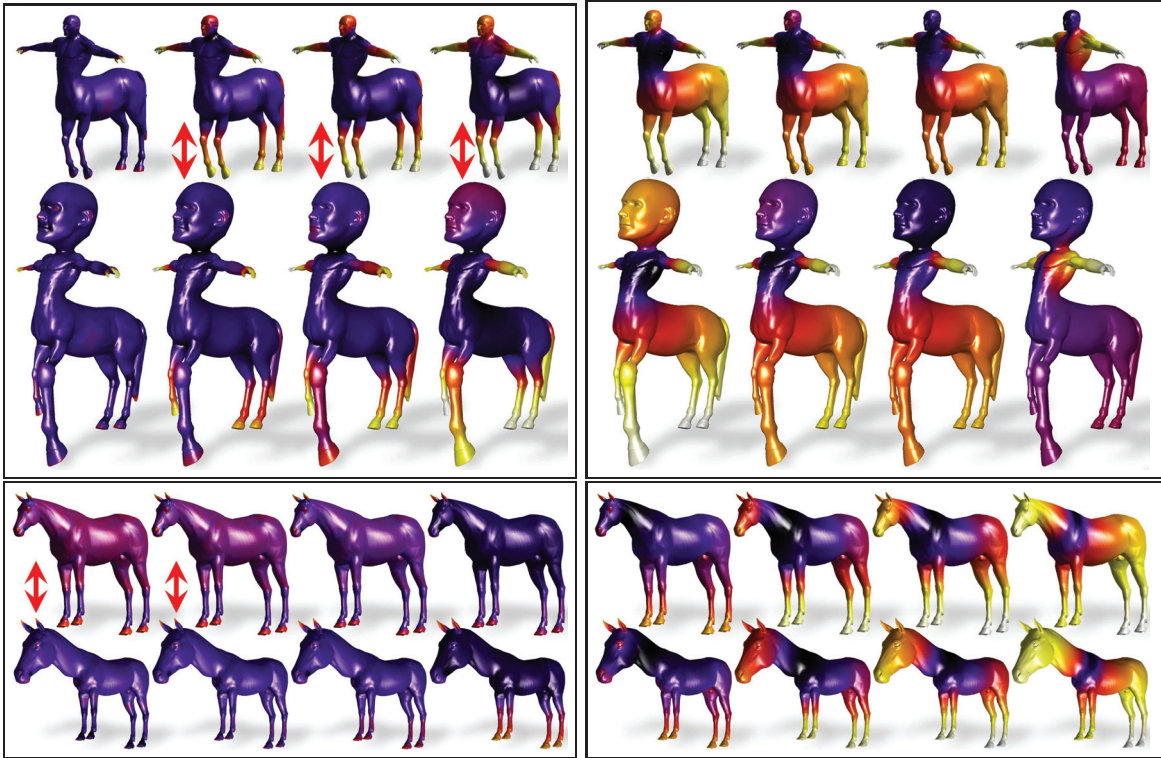


Figure 4. The HKS at different times, texture mapped onto the surface for the regular metric (left frames) and the invariant metric (right frames). The four shapes in each row, left to right, capture the HKS values at $t = 10, 50, 100,$ and $500,$ respectively.

7. Appendix: Useful notation and relations. The Laplace–Beltrami operator is defined as $\Delta_g \equiv \frac{1}{\sqrt{g}} \partial_i \sqrt{g} g^{ij} \partial_j,$ where

$$(g^{ij}) = (g_{ij})^{-1} = \frac{1}{g} \begin{pmatrix} g_{22} & -g_{12} \\ -g_{12} & g_{11} \end{pmatrix}$$

is the inverse metric matrix. The mean curvature vector can then be written as

$$2H\vec{n} = (\kappa_1 + \kappa_2)\vec{n} = \Delta_g S = \frac{1}{\sqrt{g}} \partial_i \sqrt{g} g^{ij} \partial_j S,$$

where $\partial_i \equiv \frac{\partial}{\partial w^i};$ for example, $\partial_1 = \partial_u = \frac{\partial}{\partial u}.$

For a surface given as a graph $z = f(x, y),$ we have

$$K = \frac{f_{xx}f_{yy} - f_{xy}^2}{(1 + f_x^2 + f_y^2)^2} = \frac{\det(\text{Hess}(f))}{(1 + |\nabla f|^2)^2},$$

$$H = \frac{(1 + f_{xx})f_y^2 - 2f_{xy}f_xf_y + (1 + f_{yy})f_x^2}{(1 + f_x^2 + f_y^2)^{3/2}} = \text{div} \left(\frac{\nabla f}{\sqrt{1 + |\nabla f|^2}} \right),$$

where $\text{Hess}(f)$ is the Hessian of $f(x, y).$

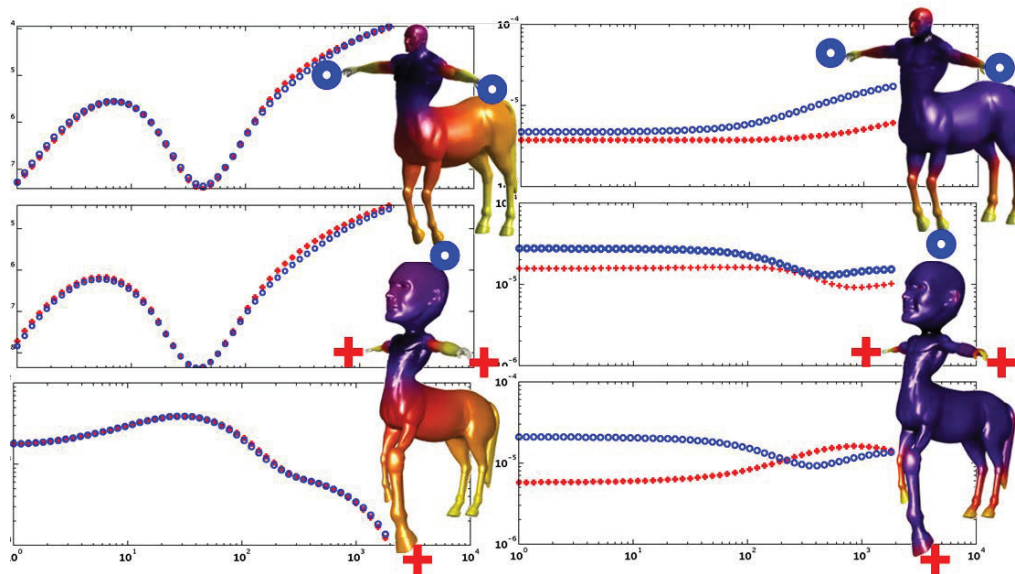


Figure 5. Scaled HKSs for the regular metric (right) and the invariant version (left). The blue circles represent the signatures for three points on the original surface, while the red plus signs are computed from the deformed version. Using a log-log axis, we plot the scaled HKS as a function of t .

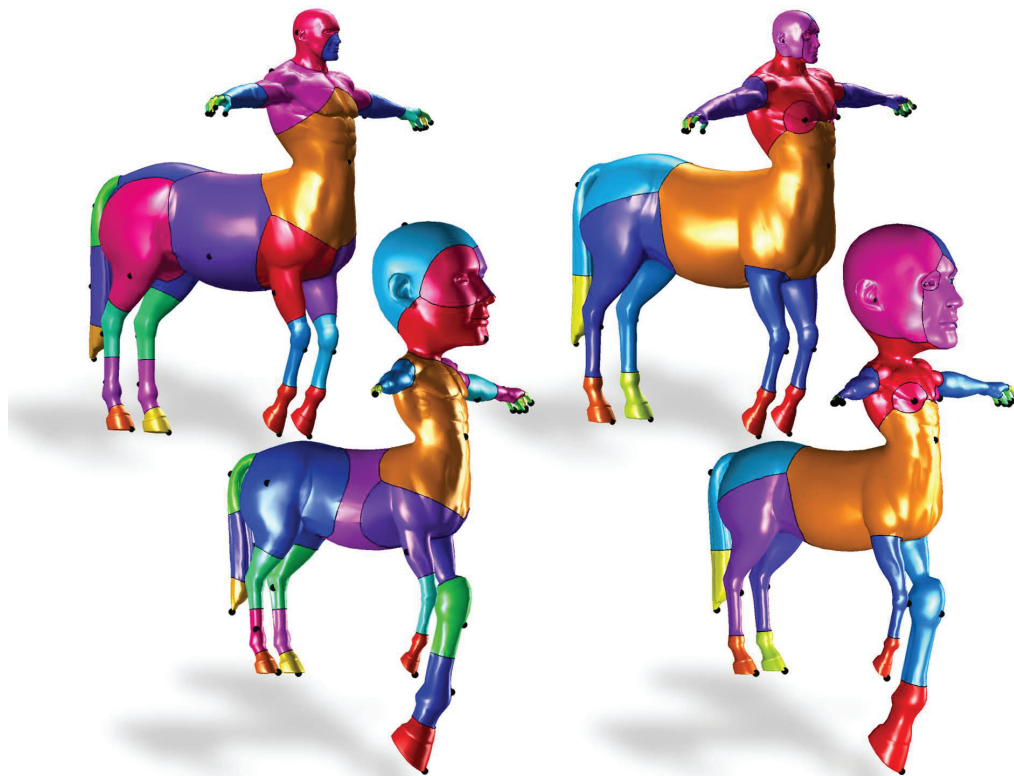


Figure 6. Voronoi diagram using diffusion distances for farthest point sampling each surface with 30 points, applying the regular metric (left two surfaces) and the invariant version (right two surfaces).

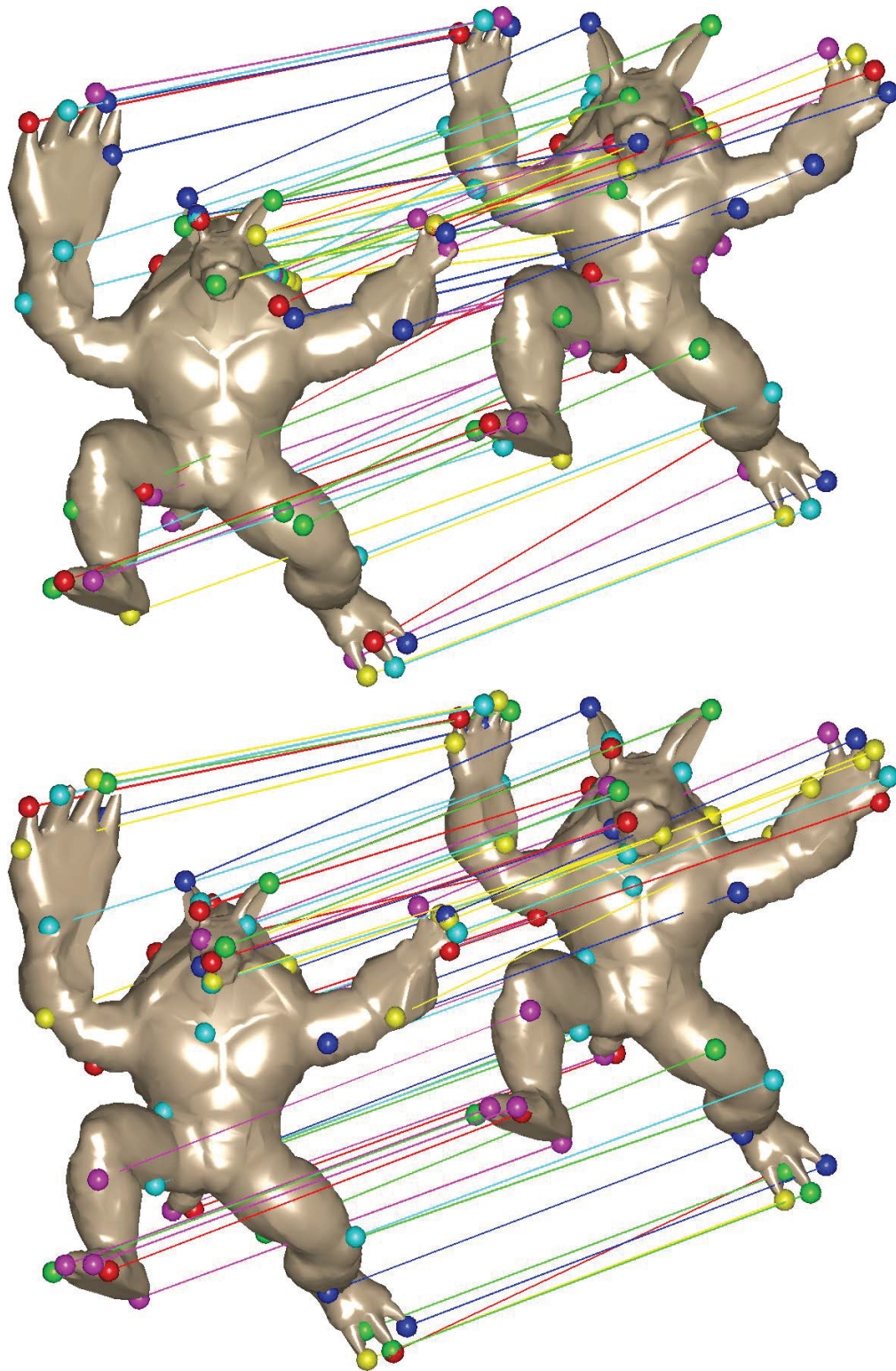


Figure 7. Using the GMDS method for surface matching with the regular metric (top) and the invariant one (bottom).

Table 1

Performance of the \tilde{g} -HKS on SHREC'10 shape retrieval benchmark with the ShapeGoogle framework (recognition rate in %).

Transformation	Strength				
	1	≤ 2	≤ 3	≤ 4	≤ 5
Isometry	100.00	100.00	100.00	97.76	97.44
Topology	100.00	100.00	100.00	98.72	97.82
Micro holes	100.00	100.00	100.00	100.00	100.00
Scale	100.00	100.00	100.00	100.00	100.00
Local scale	100.00	100.00	100.00	93.33	83.73
Noise	100.00	100.00	100.00	100.00	100.00
Shot noise	100.00	100.00	100.00	100.00	100.00

The mean curvature is given by

$$H = \frac{g_{22}b_{11} - 2g_{12}b_{12} + g_{11}b_{22}}{2g} = \frac{1}{2}b_{ij}g^{ij},$$

where $(g^{ij}) = (g_{ij})^{-1}$ is the inverse metric matrix. The two principal curvatures can now be written as functions of H and K ,

$$\begin{aligned}\kappa_1 &= H + \sqrt{H^2 - K}, \\ \kappa_2 &= H - \sqrt{H^2 - K}.\end{aligned}$$

This allows us to define other scale invariant differential forms. For example, an intrinsic measure for surfaces embedded in \mathbb{R}^3 is

$$\kappa_{\min}^2 = \min(\kappa_1^2, \kappa_2^2) = \left(\sqrt{H^2 - K} - |H|\right)^2.$$

It could be used to define an alternative isometric and scale invariant metric by

$$(7.1) \quad \check{g}_{ij} = \kappa_{\min}^2 \langle S_{\omega^i} S_{\omega^j} \rangle = \kappa_{\min}^2 g_{ij},$$

which is not explored in this paper.

REFERENCES

- [1] L. ALVAREZ, F. GUICHARD, P.-L. LIONS, AND J.-M. MOREL, *Axioms and fundamental equations of image processing*, Arch. Ration. Mech. Anal., 123 (1993), pp. 199–257.
- [2] P. BÉRARD, G. BESSON, AND S. GALLOT, *Embedding Riemannian manifolds by their heat kernel*, Geom. Funct. Anal., 4 (1994), pp. 373–398.
- [3] P. J. BESL AND N. D. MCKAY, *A method for registration of 3-D shapes*, IEEE Trans. Pattern Anal. Mach. Intell., 14 (1992), pp. 239–256.
- [4] A. M. BRONSTEIN, M. M. BRONSTEIN, U. CASTELLANI, B. FALCIDIENO, A. FUSIELLO, A. GODIL, L. J. GUIBAS, I. KOKKINOS, Z. LIAN, M. OVSJANIKOV, G. PATANÉ, M. SPAGNUOLO, AND R. TOLDO, *SHREC 2010: Robust large-scale shape retrieval benchmark*, in Proceedings of the Eurographics Workshop on 3D Object Retrieval, Norrköping, Sweden, 2010.

- [5] A. M. BRONSTEIN, M. M. BRONSTEIN, L. J. GUIBAS, AND M. OVSJANIKOV, *Shape Google: Geometric words and expressions for invariant shape retrieval*, ACM Trans. Graph., 30 (2011), 1.
- [6] A. M. BRONSTEIN, M. M. BRONSTEIN, AND R. KIMMEL, *Efficient computation of isometry-invariant distances between surfaces*, SIAM J. Sci. Comput., 28 (2006), pp. 1812–1836.
- [7] A. M. BRONSTEIN, M. M. BRONSTEIN, AND R. KIMMEL, *Expression-invariant representations of faces*, IEEE Trans. Image Process., 16 (2007), pp. 188–197.
- [8] A. M. BRONSTEIN, M. M. BRONSTEIN, AND R. KIMMEL, *Numerical Geometry of Non-Rigid Shapes*, Springer, New York, 2008.
- [9] A. M. BRONSTEIN, M. M. BRONSTEIN, R. KIMMEL, M. MAHMOUDI, AND G. SAPIRO, *A Gromov-Hausdorff framework with diffusion geometry for topologically-robust non-rigid shape matching*, Int. J. Comput. Vision, 89 (2010), pp. 266–286.
- [10] M. M. BRONSTEIN AND I. KOKKINOS, *Scale-invariant heat kernel signatures for non-rigid shape recognition*, in Proceedings of the IEEE Conference on Computer Vision and Pattern Recognition (CVPR), San Francisco, 2010, IEEE Computer Society, Washington, DC, 2010, pp. 1704–1711.
- [11] A. BROOK, A. M. BRUCKSTEIN, AND R. KIMMEL, *On similarity-invariant fairness measures*, in Scale Space and PDE Methods for Computer Vision, Lecture Notes in Comput. Sci. 3459, Springer-Verlag, Berlin, Heidelberg, 2005, pp. 456–467.
- [12] A. M. BRUCKSTEIN, R. J. HOLT, A. N. NETRAVALI, AND T. J. RICHARDSON, *Invariant signatures for planar shape recognition under partial occlusion*, CVGIP: Image Underst., 58 (1993), pp. 49–65.
- [13] A. M. BRUCKSTEIN, N. KATZIR, M. LINDENBAUM, AND M. PORAT, *Similarity-invariant signatures for partially occluded planar shapes*, Int. J. Comput. Vision, 7 (1992), pp. 271–285.
- [14] A. M. BRUCKSTEIN AND A. N. NETRAVALI, *On differential invariants of planar curves and recognizing partially occluded planar shapes*, Ann. Math. Artif. Intell., 13 (1995), pp. 227–250.
- [15] A. M. BRUCKSTEIN, E. RIVLIN, AND I. WEISS, *Scale-space local invariants*, Image Vision Comput., 15 (1997), pp. 335–344.
- [16] A. M. BRUCKSTEIN AND D. SHAKED, *Skew symmetry detection via invariant signatures*, Pattern Recogn., 31 (1998), pp. 181–192.
- [17] E. CALABI, P. J. OLVER, C. SHAKIBAN, A. TANNENBAUM, AND S. HAKER, *Differential and numerically invariant signature curves applied to object recognition*, Int. J. Comput. Vision, 26 (1998), pp. 107–135.
- [18] S. CARLSSON, R. MOHR, T. MOONS, L. MORIN, C. A. ROTHWELL, M. VAN DIEST, L. VAN GOOL, F. VEILLON, AND A. ZISSERMAN, *Semi-local projective invariants for the recognition of smooth plane curves*, Int. J. Comput. Vision, 19 (1996), pp. 211–236.
- [19] F. CHAZAL, D. COHEN-STEINER, L. J. GUIBAS, F. MÉMOLI, AND S. OUDOT, *Gromov-Hausdorff stable signatures for shapes using persistence*, Comput. Graph. Forum, 28 (2009), pp. 1393–1403.
- [20] Y. CHEN AND G. MEDIONI, *Object modelling by registration of multiple range images*, Image Vision Comput., 10 (1992), pp. 145–155.
- [21] T. COHIGNAC, C. LOPEZ, AND J. M. MOREL, *Integral and local affine invariant parameter and application to shape recognition*, in Proceedings of the 12th IAPR International Conference on Pattern Recognition (ICPR), Vol. 1, IEEE Computer Society Press, Los Alamitos, CA, 1994, pp. 164–168.
- [22] R. R. COIFMAN AND S. LAFON, *Diffusion maps*, Appl. Comput. Harmon. Anal., 21 (2006), pp. 5–30.
- [23] F. CUCKER AND S. SMALE, *On the mathematical foundations of learning*, Bull. Amer. Math. Soc., 39 (2002), pp. 1–49.
- [24] J. DIGNE, J. M. MOREL, C. M. SOUZANI, AND C. LARTIGUE, *Scale space meshing of raw data point sets*, Comput. Graph. Forum, 30 (2011), pp. 1630–1642.
- [25] G. DZIUK, *Finite elements for the Beltrami operator on arbitrary surfaces*, in Partial Differential Equations and Calculus of Variations, S. Hildebrandt and R. Leis, eds., Lecture Notes in Math. 1357, Springer, Berlin, Heidelberg, 1988, pp. 142–155.
- [26] A. ELAD AND R. KIMMEL, *On bending invariant signatures for surfaces*, IEEE Trans. Pattern Anal. Mach. Intell., 25 (2003), pp. 1285–1295.
- [27] A. B. HAMZA AND H. KRIM, *Geodesic object representation and recognition*, in Discrete Geometry for Computer Imagery, Lecture Notes in Comput. Sci. 2886, Springer, Berlin, Heidelberg, 2003, pp. 378–387.
- [28] A. B. HAMZA AND H. KRIM, *Geodesic matching of triangulated surfaces*, IEEE Trans. Image Process., 15 (2006), pp. 2249–2258.

- [29] M. HILAGA, Y. SHINAGAWA, T. KOHMURA, AND T. L. KUNII, *Topology matching for fully automatic similarity estimation of 3D shapes*, in SIGGRAPH '01, Proceedings of the 28th Annual Conference on Computer Graphics and Interactive Techniques, Los Angeles, CA, ACM, New York, 2001, pp. 203–212.
- [30] A. ION, N. M. ARTNER, G. PEYRÉ, W. G. KROPATSCH, AND L. D. COHEN, *Matching 2D and 3D articulated shapes using the eccentricity transform*, *Computer Vis. Image Underst.*, 115 (2011), pp. 817–834.
- [31] M. KILIAN, N. J. MITRA, AND H. POTTMANN, *Geometric modeling in shape space*, *ACM Trans. Graph.*, 26 (2007), 64.
- [32] R. KIMMEL, *Affine differential signatures for gray level images of planar shapes*, in Proceedings of the 13th International Conference on Pattern Recognition, Vol. 1, Vienna, Austria, 1996, IEEE Computer Society, Washington, DC, 1996, pp. 45–49.
- [33] H. LING AND D. W. JACOBS, *Using the inner-distance for classification of articulated shapes*, in Proceedings of the IEEE Computer Society Conference on Computer Vision and Pattern Recognition (CVPR), Vol. 2, San Diego, CA, 2005, pp. 719–726.
- [34] Y. LIPMAN AND T. FUNKHOUSER, *Möbius voting for surface correspondence*, *ACM Trans. Graph.*, 28 (2009), 72.
- [35] N. LITKE, M. DROSKE, M. RUMPF, AND P. SCHRÖDER, *An image processing approach to surface matching*, in SGP'05, Proceedings of the Third Eurographics Symposium on Geometry Processing, Eurographics Association, Aire-la-Ville, Switzerland, 2005, 207.
- [36] D. G. LOWE, *Distinctive image features from scale-invariant keypoints*, *Int. J. Comput. Vision*, 60 (2004), pp. 91–110.
- [37] F. MÉMOLI AND G. SAPIRO, *A theoretical and computational framework for isometry invariant recognition of point cloud data*, *Found. Comput. Math.*, 5 (2005), pp. 313–347.
- [38] M. MEYER, M. DESBRUN, P. SCHRÖDER, AND A. H. BARR, *Discrete differential-geometry operators for triangulated 2-manifolds*, in Visualization and Mathematics III, H.-C. Hege and K. Polthier, eds., Springer, Berlin, 2003, pp. 35–57.
- [39] T. MOONS, E. PAUWELS, L. J. VAN GOOL, AND A. OOSTERLINCK, *Foundations of semi-differential invariants*, *Int. J. Comput. Vision*, 14 (1995), pp. 25–48.
- [40] J.-M. MOREL AND G. YU, *ASIFT: A new framework for fully affine invariant image comparison*, *SIAM J. Imaging Sci.*, 2 (2009), pp. 438–469.
- [41] P. J. OLVER, *Joint invariant signatures*, *Found. Comput. Math.*, 1 (1999), pp. 3–67.
- [42] P. J. OLVER, *A survey of moving frames*, in Computer Algebra and Geometric Algebra with Applications, Lecture Notes in Comput. Sci. 3519, H. Li, P. J. Olver, and G. Sommer, eds., Springer-Verlag, New York, 2005, pp. 105–138.
- [43] R. OSADA, T. FUNKHOUSER, B. CHAZELLE, AND D. DOBKIN, *Shape distributions*, *ACM Trans. Graph.*, 21 (2002), pp. 807–832.
- [44] M. OVSJANIKOV, J. SUN, AND L. J. GUIBAS, *Global intrinsic symmetries of shapes*, *Comput. Graph. Forum*, 27 (2008), pp. 1341–1348.
- [45] E. PAUWELS, T. MOONS, L. J. VAN GOOL, P. KEMPENAEERS, AND A. OOSTERLINCK, *Recognition of planar shapes under affine distortion*, *Int. J. Comput. Vision*, 14 (1995), pp. 49–65.
- [46] U. PINKALL AND K. POLTHIER, *Computing discrete minimal surfaces and their conjugates*, *Experiment. Math.*, 2 (1993), pp. 15–36.
- [47] H. QIU AND E. R. HANCOCK, *Clustering and embedding using commute times*, *IEEE Trans. Pattern Anal. Mach. Intell.*, 29 (2007), pp. 1873–1890.
- [48] D. RAVIV, A. M. BRONSTEIN, M. M. BRONSTEIN, AND R. KIMMEL, *Symmetries of non-rigid shapes*, in Proceedings of the Non-rigid Registration and Tracking Workshop, IEEE 11th International Conference on Computer Vision (ICCV), 2007.
- [49] D. RAVIV, A. M. BRONSTEIN, M. M. BRONSTEIN, AND R. KIMMEL, *Full and partial symmetries of non-rigid shapes*, *Int. J. Comput. Vision*, 89 (2010), pp. 18–39.
- [50] D. RAVIV, A. M. BRONSTEIN, M. M. BRONSTEIN, R. KIMMEL, AND G. SAPIRO, *Diffusion symmetries of non-rigid shapes*, in Proceedings of the Fifth International Symposium on 3D Data Processing Visualization and Transmission (3DPVT), Paris, France, 2010.
- [51] D. RAVIV, A. M. BRONSTEIN, M. M. BRONSTEIN, R. KIMMEL, AND N. SOCHEN, *Affine-invariant diffusion geometry for the analysis of deformable 3D shapes*, in Proceedings of the 2011 IEEE Conference on Computer Vision and Pattern Recognition (CVPR), 2011, pp. 2361–2367.

- [52] D. RAVIV AND R. KIMMEL, *Affine invariant non-rigid shape analysis*, Int. J. Comput. Vision, submitted.
- [53] M. RUGGERI, G. PATANÈ, M. SPAGNUOLO, AND D. SAUPE, *Spectral-driven isometry-invariant matching of 3D shapes*, Int. J. Comput. Vision, 89 (2010), pp. 248–265.
- [54] J. RUGIS AND R. KLETTE, *A scale invariant surface curvature estimator*, in Advances in Image and Video Technology, Lecture Notes in Comput. Sci. 4319, Springer-Verlag, Berlin, Heidelberg, 2006, pp. 138–147.
- [55] R. M. RUSTAMOV, *Laplace-Beltrami eigenfunctions for deformation invariant shape representation*, in SGP '07, Proceedings of the Fifth Eurographics Symposium on Geometry Processing, Barcelona, Spain, 2007, Eurographics Association, Aire-La-Ville, Switzerland, 2007, pp. 225–233.
- [56] G. SAPIRO, *Affine Invariant Shape Evolutions*, Ph.D. thesis, Technion—IIT, Haifa, Israel, 1993.
- [57] J. SUN, M. OVSJANKOV, AND L. J. GUIBAS, *A concise and provably informative multi-scale signature based on heat diffusion*, Comput. Graph. Forum, 28 (2009), pp. 1383–1392.
- [58] L. J. VAN GOOL, M. H. BRILL, E. B. BARRETT, T. MOONS, AND E. PAUWELS, *Semi-differential invariants for nonplanar curves*, in Geometric Invariance in Computer Vision, J. Mundy and A. Zisserman, eds., MIT Press, Cambridge, MA, 1992, pp. 293–309.
- [59] L. J. VAN GOOL, T. MOONS, E. PAUWELS, AND A. OOSTERLINCK, *Semi-differential invariants*, in Geometric Invariance in Computer Vision, J. Mundy and A. Zisserman, eds., MIT Press, Cambridge, MA, 1992, pp. 157–192.
- [60] O. VAN KAICK, H. ZHANG, G. HAMARNEH, AND D. COHEN-OR, *A survey on shape correspondence*, Comput. Graph. Forum, 30 (2011), pp. 1681–1707.
- [61] Y. WANG, M. GUPTA, S. ZHANG, S. WANG, X. GU, D. SAMARAS, AND P. HUANG, *High resolution tracking of non-rigid motion of densely sampled 3D data using harmonic maps*, Int. J. Comput. Vision, 76 (2008), pp. 283–300.
- [62] M. WARDETZKY, S. MATHUR, F. KÄLBERER, AND E. GRINSPUN, *Discrete Laplace operators: No free lunch*, in SGP '07, Proceedings of the Fifth Eurographics Symposium on Geometry Processing, Eurographics Association, Aire-la-Ville, Switzerland, 2007, pp. 33–37.
- [63] I. WEISS, *Projective Invariants of Shapes*, Technical report CAR-TR-339, Center for Automation, University of Maryland, College Park, MD, 1988.
- [64] G. WOLANSKY, *Incompressible, quasi-isometric deformations of 2-dimensional domains*, SIAM J. Imaging Sci., 2 (2009), pp. 1031–1048.
- [65] Z. XU AND G. XU, *Discrete schemes for Gaussian curvature and their convergence*, Comput. Math. Appl., 57 (2009), pp. 1187–1195.
- [66] A. ZAHARESCU, E. BOYER, K. VARANASI, AND R. HORAUD, *Surface feature detection and description with applications to mesh matching*, in Proceedings of the IEEE Conference on Computer Vision and Pattern Recognition (CVPR), IEEE Computer Society, Los Alamitos, CA, 2009, pp. 373–380.